INTERFACE

royalsocietypublishing.org/journal/rsif

Research

Cite this article: Haluts A, Jordan A, Gov NS. 2023 Modelling animal contests based on spatio-temporal dynamics. *J. R. Soc. Interface* **20**: 20220866. https://doi.org/10.1098/rsif.2022.0866

Received: 1 December 2022
Accepted: 25 April 2023

Subject Category:
Life Sciences–Physics interface

Subject Areas:
biophysics, computational biology

Keywords:
animal contests, agonistic interactions, assessment strategy, resource holding potential, effective interaction forces, physics-inspired modelling

Author for correspondence:
Amir Haluts
e-mail: halutsamir@gmail.com

Electronic supplementary material is available online at https://doi.org/10.6084/m9.figshare.c.6659079.

THE ROYAL SOCIETY PUBLISHING

Modelling animal contests based on spatio-temporal dynamics

Amir Haluts[1], Alex Jordan[2] and Nir S. Gov[1]

[1]Department of Chemical and Biological Physics, Weizmann Institute of Science, Rehovot 7610001, Israel
[2]Department of Collective Behavior, Max Planck Institute of Animal Behavior, Konstanz 78315, Germany

AH, 0000-0001-8052-9534; AJ, 0000-0001-6131-9734; NSG, 0000-0001-7774-1139

We present a general theoretical model for the spatio-temporal dynamics of animal contests. Inspired by interactions between physical particles, the model is formulated in terms of effective interaction potentials, which map typical elements of contest behaviour into empirically verifiable rules of contestant motion. This allows us to simulate the observable dynamics of contests in various realistic scenarios, notably in dyadic contests over a localized resource. Assessment strategies previously formulated in game-theoretic models, as well as the effects of fighting costs, can be described as variations in our model's parameters. Furthermore, the trends of contest duration associated with these assessment strategies can be derived and understood within the model. Detailed description of the contestants' motion enables the exploration of spatio-temporal properties of asymmetric contests, such as the emergence of chase dynamics. Overall, our framework aims to bridge the growing gap between empirical capabilities and theory in this widespread aspect of animal behaviour.

1. Introduction

Contests over limited resources are a common feature of animal behaviour, and have been the focus of many empirical and theoretical works over the past decades [1]. Due to the cost and benefit trade-offs that they entail, and following the foundations laid by the seminal works of the 1970s [2 6], animal contests were predominantly modelled within the framework of game theory [7 10]. Although they can generate empirically testable predictions notably trends of contest duration and escalation [11], experimental verification of game-theoretic contest models remains elusive [11 14], as empirical studies rarely yield more than anecdotal evidence in support of a particular class of models or the rejection of another [11,13,14]. Moreover, the theoretical foundations of these models are typically stated in terms of how contestants gather information about their own and their rival's 'resource holding potential' (RHP) [7 10,15 19], a generally defined measure for the ability to obtain and defend resources [5] that can rarely be measured directly. These difficulties have sparked disagreement over best practice in measuring animal contests [12,14,20 22], and highlight the fact that most contest models meet the observable dynamics of contest behaviour only in their endpoint predictions and ignore the detailed dynamics of contests in real time and space. This makes direct comparison of theoretical contest games with real animal contests inherently difficult.

The most striking aspect of animal contests is the spatial dynamics of contestants as they react to real-time inputs. Importantly, the spatial dynamics of contests are directly measurable, and nowadays can be readily tracked [23,24]. Although seemingly intricate and diverse [25], these dynamics commonly involve stereotypical behavioural elements that characterize contests in many species [1,25,26]. Another central element is a spatially localized resource, commonly a mate [27,28] or territory [29], which attracts potential rivals and drives them into contest range. Once the contestants are engaged in an interaction, their spatial dynamics are governed by behavioural elements that typify agonistic encounters, such as displays, attacks and retreats [25]. These features of animal contests can be described as universal rules of contestant motion, which, we propose, can then be associated with effective interaction forces that encode the contestants' behaviour, as we have recently shown for a system of spider contestants [30]. This approach yielded new mechanistic explanations for previous observations regarding the competitive advantage of larger contestants [30]. Similar methods have been applied to model inter-agent interactions in animal groups in the context of collective behaviour [31 36]. This motivates us to propose a new theoretical framework for the observable dynamics of animal contests, which relies on generic and broadly applicable rules of inter-contestant interactions.

In this work, we construct a general theoretical model for the spatial and temporal dynamics of animal contests. The model is formulated in terms of effective interaction potentials, which map typical elements of contest behaviour into rules of attraction and repulsion between contestants, and are analogous to the potential interaction energies between physical particles. Through the effective interaction forces that they generate, these potentials govern the motion of contestants as they interact with each other and with a localized resource. This fundamental framework is used to simulate the spatio-temporal dynamics of our model's contestants in dyadic contests. Using simulated data, we demonstrate how our model's interaction potentials can be measured empirically in any system in which contest dynamics can be observed.

The scope of this general framework goes far beyond that of our motivating special case [30]. We show that the previously proposed RHP-assessment strategies [7 10,15 19], which are stated in terms of how contestants gather information about their own and their rival's RHP, can be described as variations in the model's parameters. This is done by introducing an 'assessment function', which can describe various modes of assessment within its continuous parameter space. Further extending the relation between the model's parameters and the underlying behaviour, we account for fighting costs. Using the model's representation of the well-studied self- and mutual assessment strategies [11], we show that the RHP-dependent trends of contest duration associated with these assessment strategies can be derived and understood within our model as an emergent property of contest dynamics. Finally, we explore spatio-temporal properties of asymmetric contests between RHP-unmatched contestants. These results showcase the applicability of the model to various realistic contest scenarios, in which the comparison between theory and experiment can be facilitated by the analysis of spatio-temporal data derived from the contestants' trajectories.

2. The basic model: construction and measurement

2.1. Effective interaction potentials

Our model is based on the mapping of typical contest behaviour to generic rules of inter-contestant interactions. These rules are encoded by effective 'contestant interaction potentials' $V_{j\to i}$, which capture the influence of a rival contestant j on the motion of contestant i (figure 1*a*,*b*). Not to be confused with RHPs, our interaction potentials are analogous to the potential interaction energies that govern the interactions between physical particles. We construct these potentials based on the following generic features of contest behaviour, which we state in terms of effective attraction or repulsion between contestants i and j depending on the distance between them: (i) long-range repulsion due to mutual avoidance (which can be surmounted due to an attracting resource, as shown in figure 1*c*,*d*), (ii) medium- to short-range attraction when the contestants reach a separation distance in which conflict escalation is inevitable (and hence move towards each other), (iii) strong repulsion at contact, and (iv) the strength of the interaction decays to zero when the contestants are far apart. Note that the tendency to decrease the inter-contestant distance (effective attraction) is associated here with conflict escalation, while the tendency to increase this distance (effective repulsion) is associated with de-escalation. These effects can be directly measured in experiments, as we demonstrate in a later section.

Various interaction potentials can be constructed to satisfy the above requirements, that is to have a qualitative shape as in figure 1*a*,*b*. Here, we propose one such particular potential, a combination of a logarithmic repulsion and an attractive Gaussian well, for which the extrema can be obtained analytically (electronic supplementary material, S1),

$$V_{j\to i}(x_{ij}) = \quad \alpha_{j\to i}\exp(\quad \beta x_{ij}^2) \quad \delta_{j\to i}\ln(x_{ij}), \qquad x_{ij} = \frac{|\mathbf{r}_i \quad \mathbf{r}_j|}{x_0}, \tag{2.1}$$

where x_{ij} is the (dimensionless) distance between contestants i and j (with respective position vectors $\mathbf{r}_i$ and $\mathbf{r}_j$), $\alpha_{j\to i}$ and $\delta_{j\to i}$ are positive 'interaction parameters' that set the strengths of effective attraction and repulsion (experienced by i when interacting with a rival j), $\beta > 0$ determines the range of effective attraction, and x_0 is a length scale distance parameter. Both β and x_0 are assumed to be the same for all contestants in a given system, and in this work will be set to equal 1. Electronic supplementary material, S2 addresses the addition of an intermediate 'evaluation' regime, which has been observed in various animal contests [7,17,30,37], to $V_{j\to i}$, demonstrating the inclusion of other (system-specific) features in this interaction potential. The same approach can account for the spatio-temporal characteristics of any contest behaviour that occurs at a typical inter-contestant distance. An omnipresent example for such behaviours is agonistic displays [38 41].

Note that $\alpha_{j\to i}$ reflects the motivation of contestant i to escalate the interaction (that is, how aggressive i is) and is, therefore, associated with the (absolute or relative) RHP of i, while $\delta_{j\to i}$ reflects how intimidating (repulsive) the rival j is perceived by i, and is, therefore, associated with the (absolute or relative) RHP of j. In a later section, we construct an explicit functional relationship between the parameters $\alpha_{j\to i}$ and $\delta_{j\to i}$ and the contestants' RHPs depending on the assessment strategy that they employ. An analogous interaction potential $V_{i\to j}$ (with interaction parameters $\alpha_{i\to j}$ and $\delta_{i\to j}$) is experienced by the rival j due to the interaction with i and, as implied by the directional arrow notation, in general $V_{j\to i} \neq V_{i\to j}$ since these potentials manifest asymmetries between the contestants (as illustrated in figure 1*e*). The influence of $V_{j\to i}$ and $V_{i\to j}$ on the motion of the contestants

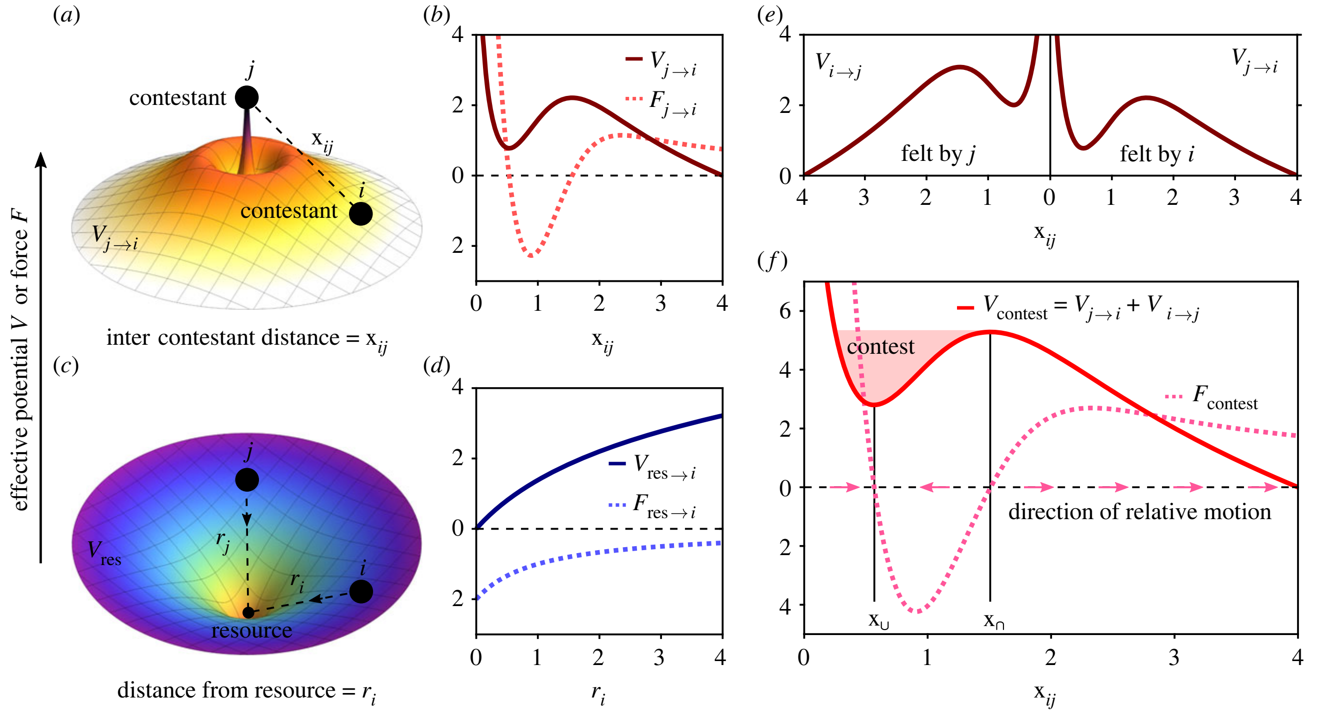

Figure 1. Effective interaction potentials. (*a*) The landscape of the effective 'contestant interaction potential' $V_{j\to i}$, as given in equation (2.1), with interaction parameters $\alpha_{j\to i}=7$, $\delta_{j\to i}=3$ and $\beta=1$. (*b*) The profiles of $V_{j\to i}$ and its corresponding force $F_{j\to i}=-\mathrm{d}V_{j\to i}/\mathrm{d}x_{ij}$ as a function of the inter-contestant distance x_{ij}. The graph of $V_{j\to i}$ was shifted vertically such that the lowest shown point has a 'height' of zero. Parameter values as in (*a*). (*c*) The landscape of an effective 'resource potential' V_{res} with a simple radially symmetrical form. Resources act as attracting regions in space that drive contestant into conflict range. (*d*) The profiles of $V_{\text{res}\to i}$ and its corresponding force $F_{\text{res}\to i}=-\mathrm{d}V_{\text{res}\to i}/\mathrm{d}r_i$ as a function of the distance from the resource $r_i=|\mathbf{r}_i|$. (*c*,*d*) The potential $V_{\text{res}\to i}(\mathbf{r}_i)=p_i\ln(r_i+\epsilon)$, where $p_i>0$ sets the attractiveness of the resource (as perceived by contestant *i*), and $\epsilon>0$ prevents divergence at the resource (defined as the origin), with $p_i=4$ and $\epsilon=1$. (*e*) Asymmetries between contestants are manifested by their contestant interaction potentials (in general $V_{j\to i}\neq V_{i\to j}$). Here, $V_{j\to i}$ is the same as in (*b*), and $V_{i\to j}$ is shown with $\alpha_{i\to j}=8$, $\delta_{i\to j}=4$ and $\beta=1$. (*f*) The relative 'contest force' $F_{\text{contest}}=F_{j\to i}+F_{i\to j}$ governs the relative motion along the inter-contestant axis (arrows). This force is associated with a relative 'contest potential' $V_{\text{contest}}=V_{j\to i}+V_{i\to j}$, which has its local maximum ($x_\cap$) and minimum ($x_\cup$) where $F_{\text{contest}}=0$ (no relative motion between the contestants). The distance $x_{ij}=x_\cap$ is defined as the contest onset.

is governed by the non-reciprocal forces that they generate, $F_{j\to i}=-\mathrm{d}V_{j\to i}/\mathrm{d}x_{ij}$ and $F_{i\to j}=-\mathrm{d}V_{i\to j}/\mathrm{d}x_{ij}$.

Access to limited resources is the primary motivation of animals to engage in contests in the first place [1]. Most of these resources, notably mates, food and territories, are inherently spatially localized, and therefore act as attracting regions in space that drive competitors closer to each other until conflict is inevitable. The level of attraction towards a given resource is determined by the perceived resource value, which could vary not only according to an absolute scale, but also between contestants and contexts [10]. We model the influence of a localized resource on the motion of contestant *i* as an effective 'resource potential' $V_{\text{res}\to i}$. As with $V_{j\to i}$, $V_{\text{res}\to i}$ should not be confused with the concept of RHP, but rather should be thought of as the effective 'energy' landscape created by the resource. The particular shape of the resource potential's landscape may be system-specific [30], but its global qualitative effect is generic: to bring contestants into contest range due to their mutual attraction to the resource. A resource potential with a simple radially symmetrical form is shown in figure 1*c*,*d*. Note that the effective potential landscapes of figure 1*a*,*c* describe interactions in a two-dimensional (planar) space, but the model is equally applicable in three dimensions.

Once contestants become strongly engaged in a contest interaction, their attention is predominantly given to their rival until the encounter is resolved. This implies an 'attention switch' in the interactions with a resource and with rivals, where the contestants' motion is significantly affected by their attraction to the resource (i.e. by $V_{\text{res}\to i}$ and $V_{\text{res}\to j}$) only when they are relatively far apart, and is dominated by their interaction with each other (i.e. by $V_{j\to i}$ and $V_{i\to j}$) when they are within the contest range. This attention switch can be expressed by the total effective potential experienced by contestant *i*, $V_{\text{tot}\to i}$, which combines the influence of a rival *j* and of a resource on the motion of contestant *i*,

$$V_{\text{tot}\to i}(\mathbf{r}_i,\mathbf{r}_j)\\ \begin{cases} V_{\text{res}\to i}(\mathbf{r}_i)+V_{j\to i}(x_{ij}), & x_{ij}\geq x_\cap \text{ (attention to resource + rival)}\\ V_{j\to i}(x_{ij}), & x_{ij}<x_\cap \text{ (attention to rival)} \end{cases} \tag{2.2}$$

where $x_\cap$ is the contest onset distance, as defined below and in figure 1*f*. A respective total effective potential $V_{\text{tot}\to j}$ is experienced by the rival *j* due to contestant *i* and the resource. Below we demonstrate how these potentials can be extracted from contest trajectories, and in [30] we demonstrate their extraction in a specific system of spider contestants, where the resource potential has a non-trivial shape.

2.2. Definition of a contest

In order to clearly define the onset of a 'contest' in our model, we consider the relative motion between the contestants along the inter-contestant axis (figure 1*a*) due only to $V_{j\to i}$ and $V_{i\to j}$. Note that according to equation (2.1), this relative motion depends only on the distance between the contestants, and is governed by the effective forces $F_{j\to i}$ and $F_{i\to j}$. Taking the $j\to i$ direction as the 'positive' direction $\hat{\mathbf{x}}_{ij} = (\mathbf{r}_i - \mathbf{r}_j)/|\mathbf{r}_i - \mathbf{r}_j|$, and the position of contestant j as a fixed point of reference, contestant i appears to be driven along $\hat{\mathbf{x}}_{ij}$ by a relative 'contest force' F_{contest}, given by

$$\begin{aligned} F_{\mathrm{contest}}(\mathrm{x}_{ij}) &= F_{j\to i}(\mathrm{x}_{ij}) + F_{i\to j}(\mathrm{x}_{ij}) \\ &= -\frac{\mathrm{d}}{\mathrm{dx}_{ij}}[V_{j\to i}(\mathrm{x}_{ij}) + V_{i\to j}(\mathrm{x}_{ij})], \end{aligned} \tag{2.3}$$

where note that the sum is taken since $F_{i\to j}$, which is applied by i on j in the $-\hat{\mathbf{x}}_{ij}$ direction, appears to drive i relative to j in the opposing $+\hat{\mathbf{x}}_{ij}$ direction. Equation (2.3) motivates the definition of a relative 'contest potential' V_{contest} as the sum of the individual interaction potentials,

$$V_{\mathrm{contest}}(\mathrm{x}_{ij}) = V_{j\to i}(\mathrm{x}_{ij}) + V_{i\to j}(\mathrm{x}_{ij}), \tag{2.4}$$

such that $F_{\mathrm{contest}} = -\mathrm{d}V_{\mathrm{contest}}/\mathrm{dx}_{ij}$. We use equations (2.3) and (2.4) to define the onset of a contest according to the direction of relative motion, which changes at the locations of the local maximum ($\mathrm{x}_\cap$) and minimum ($\mathrm{x}_\cup$) of V_{contest} (see electronic supplementary material, S1 for the analytic expressions of these extrema). When the contestants reach a separation x_{ij} that is shorter than $\mathrm{x}_\cap$, the relative force becomes attractive ($F_{\mathrm{contest}} < 0$) towards $\mathrm{x}_\cup$, and the interaction is governed by a transient bounded state (see figure 1*f*). This bounded state is equivalent to the ultimate escalation into a short-range contest, in which the contestants are completely engaged with each other. We, therefore, define $\mathrm{x}_\cap$ as the contest onset distance, and regard two contestants as engaged in a contest when $\mathrm{x}_{ij} < \mathrm{x}_\cap$ (figure 1*f*). Note that according to the particular choice of equation (2.1), the relative contest potential is given by

$$V_{\mathrm{contest}}(\mathrm{x}_{ij}) = -(\alpha_{j\to i} + \alpha_{i\to j})\exp(-\beta \mathrm{x}_{ij}{}^2) - (\delta_{j\to i} + \delta_{i\to j})\ln(\mathrm{x}_{ij}). \tag{2.5}$$

To simulate the dynamics of our model's contestants, we treat them as Brownian particles moving in space under the influence of an external potential [42], as described in electronic supplementary material, S3. Note that in this work, all contests were simulated in a two-dimensional (planar) space. Figure 2*a*–*c* describes typical trajectories of a simulated symmetric interaction between two identical contestants ($V_{j\to i} = V_{i\to j}$), where the attraction of both contestants to the resource brings them into contest range.

2.3. Extracting interaction potentials from empirical measurements

Using simulated contestant trajectories as in figure 2*a*, for which the underlying potentials are known, we demonstrate how the contestants' effective interaction potentials can be extracted from the spatio-temporal dynamics of contests. These potentials govern the velocity at which the contestants tend to move with respect to one another depending on their position. With minimal *a priori* assumptions about the observed interactions, this relative motion can be gauged by the averaged relative velocity between the contestants as a function of x_{ij},

$$v_{\mathrm{rel}}(\mathrm{x}_{ij}) = \mathrm{mean}\left(\frac{\Delta \mathrm{x}_{ij}}{\Delta \mathrm{t}}(\mathrm{x}_{ij})\right), \tag{2.6}$$

where note that $v_{\mathrm{rel}} > 0$ (a tendency to increase x_{ij}) indicates effective repulsion between the contestants, while $v_{\mathrm{rel}} < 0$ (a tendency to decrease x_{ij}) indicates effective attraction. Figure 2*d* shows the relative velocity profile described by v_{rel}, as calculated from the trajectories of $n = 30$ simulated contests as in figure 2*a*. To be informative, v_{rel} requires sufficient sampling, such that the stochastic components of the motion are mostly averaged out, and that the sampled contests are comparable, so that the remaining averaged dynamics represents the data well. For example, the relative velocity profile of figure 2*d* represents a fairly large but experimentally feasible set of RHP-matched contests with the same initial set-up (comparable contests).

Then, an averaged relative interaction potential can be derived from v_{rel} by integration with respect to x_{ij},

$$\eta V_{\mathrm{rel}}(\mathrm{x}_{ij}) \approx -\int_0^{\mathrm{x}_{ij}} v_{\mathrm{rel}}(\mathrm{x}'_{ij})\,\mathrm{dx}'_{ij}, \tag{2.7}$$

where the 'integral' denotes the approximate cumulative integration over the discrete values of the measured v_{rel} (see electronic supplementary material, S4 for the formal definition). Equation (2.7) assumes that the effects of the contestants' inertia can be neglected *on average*, such that the averaged relative velocity is directly proportional (through the 'mobility' η, see electronic supplementary material, S3) to the effective relative force associated with V_{rel}. In practice, η can be simply absorbed into V_{rel} by setting $\eta = 1$. Figure 2*d* shows the result of this integration, and electronic supplementary material, S4 describes the full practical implementation of equations (2.6) and (2.7) to a set of contest trajectories.

Although the overall shape of the observed potential V_{rel} is in good qualitative agreement with the actual contest potential, it includes contributions from the residual attraction of both contestants towards the resource, and therefore cannot be strictly identified with V_{contest}. By observing the typical contest behaviour of the studied animals, one should be able to estimate the average inter-contestant distance at which the 'attention switch' of equation (2.2) comes into play, and thereby estimate the range of x_{ij} within which the interaction is dominated by V_{contest} and the effect of the resource is negligible. For example, a clear change of the averaged relative motion from effective repulsion to effective attraction, as indicated by a sign change of v_{rel}, is a possible indicator for the onset of this range. In this range, a model for V_{contest} can be fitted to V_{rel} (electronic supplementary material, S4), as illustrated in figure 2*e*. With the $n = 30$ simulated trajectories used here, a fit according to equation (2.5) deviates only slightly from the actual V_{contest}. In the context of contest experiments, one should also be mindful when analysing trajectories of contests that occur in the presence of spatial constraints, notably those of staged contests inside bounded experimental arenas (such as tanks and pens), so as to minimize the effects of such constraints on the extraction and interpretation of the underlying interaction. This could be done, for example, by constructing arenas that are sufficiently large and by considering only trajectory fragments that are well away from a boundary.

Finally, for contests between RHP-matched contestants as in the current example, the fitted V_{contest} can be simply divided by 2 to obtain the contestant interaction potentials $V_{j\to i}$ and $V_{i\to j}$, as shown in figure 2*f*. Otherwise, a relation

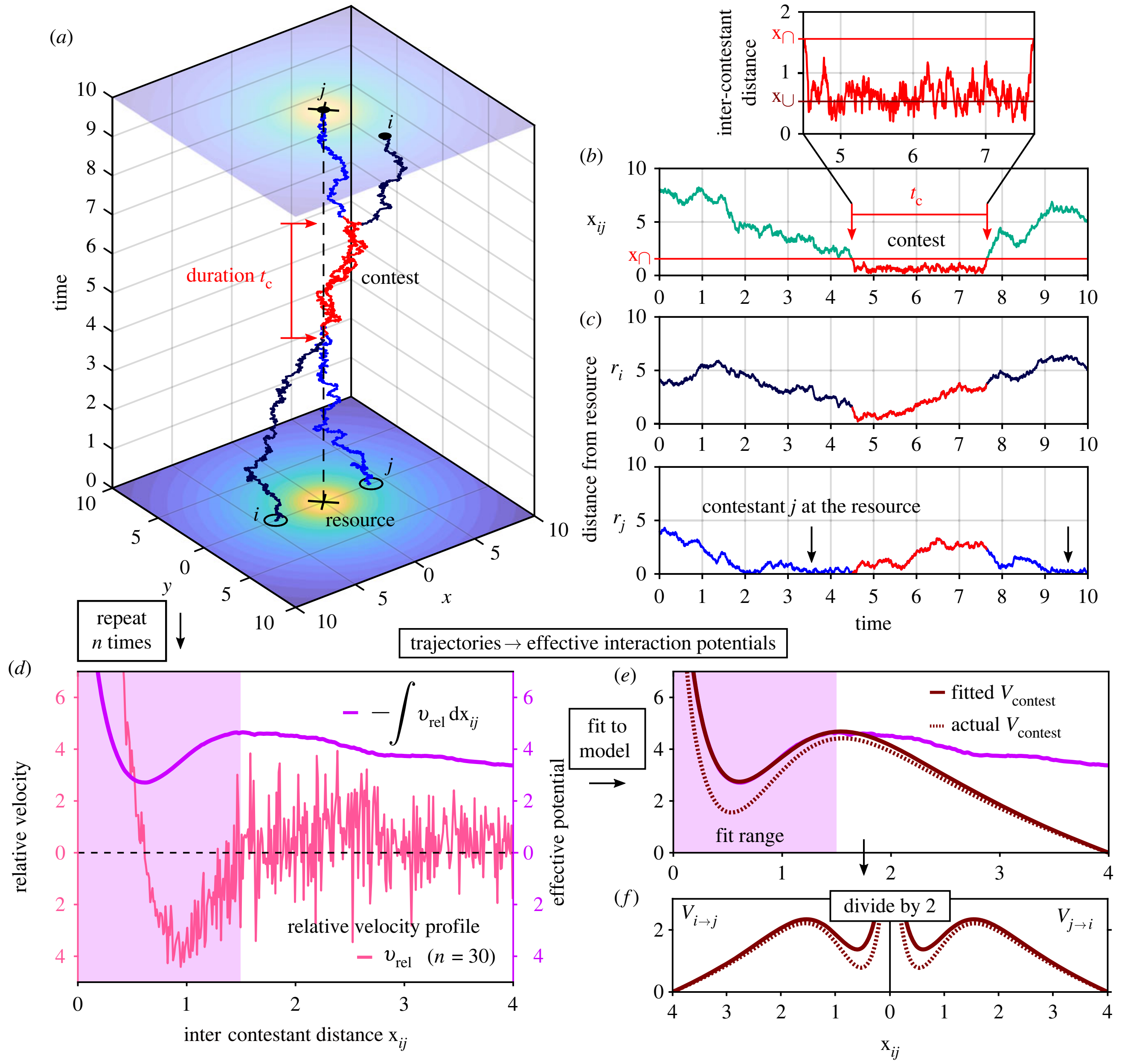

Figure 2. (*a–c*) Contestant dynamics. (*a*) Typical simulated trajectories of two identical contestants ($V_{j\to i} = V_{i\to j}$) in the vicinity of a resource. Each contestant's dynamics was simulated using electronic supplementary material, equation (S9), with $\eta = 1$ and $D = 0.5$ (see electronic supplementary material, S3), and $V_{tot\to i}$ as defined in equation (2.2), with $V_{j\to i}$ and V_{res} as in figure 1*a*,*c*, respectively. The contestants were initialized at equivalent positions on opposing sides of the resource, with $\mathbf{r}_i(t = 0) = (-4, 0)$ and $\mathbf{r}_j(t = 0) = (4, 0)$, as marked by the empty circles in the *x–y* plane. Segments of the trajectories in which the contestants were engaged in a contest ($x_{ij} < x_\cap$) are shown in red. (*b*) The distance between the contestants throughout the simulation. The tendency of the contestants to get closer to each other due to their mutual attraction to the resource brings them into contest range. As evident in the close-up view, the contestants spend the majority of the contest near the minimum, $x_\cup$, of the contest potential $V_{contest}$. (*c*) The distance between each contestant and the resource (the origin) throughout the simulation. In this particular instance, contestant *j* reached the resource before the contest, and regained it after the contest. (*d–f*) *Extracting interaction potentials from trajectories.* (*d*) The averaged relative velocity profile v_{rel} and the observed relative potential V_{rel} obtained by integration, as calculated from the trajectories of $n = 30$ simulated contests as in (*a*). The shaded rectangle marks the fit range used in (*e*). (*e*) Fit of the model's contest potential to V_{rel} within the range dominated by $V_{contest}$. This fit deviates only slightly from the actual $V_{contest}$. (*f*) For these symmetric contests, the fitted $V_{contest}$ is simply divided by 2 to obtain $V_{j\to i}$ and $V_{i\to j}$. See also electronic supplementary material, S4.

between the contestants' RHP and the parameters of the interaction potentials (an RHP-assessment strategy) has to be assumed in order to dissect $V_{contest}$ into $V_{j\to i}$ and $V_{i\to j}$. To avoid such *a priori* assumptions about the underlying assessment strategy, we propose that the initial extraction of effective interaction potentials should always rely on contests sampled from an RHP-uniform pool of contestants, e.g. contestants of similar sizes in systems where size is strongly correlated with RHP. Once effective interaction potentials are established for these RHP-matched contestants, evidence for the assessment strategy can be gathered, based on the theory developed in the following section, by sampling contests between contestants of other RHPs.

3. Integrating assessment and costs

3.1. The assessment function

The type of RHP-related information used by contestants to resolve contests, commonly termed the 'RHP-assessment strategy', has been widely used to classify contests in different species [11,43]. Historically, theoretical and empirical studies have analysed and classified animal contests according to two main categories of assessment: self-assessment, in which contestants only consider their own RHP and do not gather information about their rival's RHP [11], and mutual assessment, in which contestants consider both their own and their rival's RHP in their decision-making [11]. Existing game-theoretic models of contest behaviour were mostly constructed according to a specific assessment strategy of either the self- or mutual assessment categories, and this often limits their applicability only to systems which closely follow their underlying assessment paradigm [14].

Here, we propose that any mode of assessment can be expressed in terms of how the parameters $\alpha_{j\to i}$ and $\delta_{j\to i}$ of equation (2.1) vary with the contestants' RHP. We assume that the RHP of contestants i and j can be sufficiently expressed by single numeric variables, respectively denoted m_i and m_j. Henceforth, we will often refer to m_i and m_j as the contestants' (effective) sizes, although in general RHP is not strictly interchangeable with size [5]. Nevertheless, any metric or proxy of RHP that can be numerically expressed is compatible with this approach. In order to facilitate comparisons across taxa and scales, it is useful to define

$$m_i = \frac{\text{RHP of contestant } i}{\text{RHP of reference}}, \tag{3.1}$$

such that m_i and m_j are dimensionless effective 'sizes' that express the RHP of the contestants relative to some chosen reference in the population of interest, e.g. the estimated average.

We construct an 'assessment function' $\mathbf{A}_{j\to i}$ (of contestant i with respect to a rival j) which can express, in principle, any assessment strategy. For a two-component interaction potential as in equation (2.1), $\mathbf{A}_{j\to i}$ can be represented as a two-element vector that defines the functional relationship between the parameters $\alpha_{j\to i}$ and $\delta_{j\to i}$ and the effective size variables m_i and m_j. As explained above, $\alpha_{j\to i}$ is directly associated with the (absolute or relative) size of contestant i, while $\delta_{j\to i}$ is directly associated with the (absolute or relative) size of the rival j, and these features can be expressed by $\mathbf{A}_{j\to i}$ as follows:

$$\mathbf{A}_{j\to i}(m_i, m_j) = \begin{pmatrix} \alpha_{j\to i} \\ \delta_{j\to i} \end{pmatrix} = \begin{pmatrix} \alpha_0\, m_i^{\,s} (m_i/m_j)^{s_Q} \\ \delta_0\, m_j^{\,r} (m_j/m_i)^{r_Q} \end{pmatrix}, \tag{3.2}$$

where α_0 and δ_0 are scaling parameters, and the different RHP-dependent components represent: $m_i^{\,s}$ absolute self-assessment; $m_j^{\,r}$ absolute rival-assessment; $(m_i/m_j)^{s_Q}$ and $(m_j/m_i)^{r_Q}$ relative self- and rival-assessment (mutual assessment), respectively. Note that the opponent's assessment function, $\mathbf{A}_{i\to j} = (\alpha_{i\to j}, \delta_{i\to j})$, is obtained by swapping the functional roles of m_i and m_j in equation (3.2). The assessment strategy, which is now defined in terms of how $\alpha_{j\to i}$ and $\delta_{j\to i}$ vary with m_i and m_j, is represented by the (non-negative) values of the exponents s, r, s_Q, r_Q. In particular, we propose that 'pure' self-assessment can be described by $s > 0$ and r, s_Q, $r_Q = 0$, that is

$$\mathbf{A}_{j\to i}(m_i, m_j) = \begin{pmatrix} \alpha_0\, m_i^{\,s} \\ \delta_0 \end{pmatrix} \quad \text{for pure self-assessment,} \tag{3.3}$$

and that 'pure' mutual (relative) assessment can be described by s, $r = 0$ and s_Q, $r_Q > 0$, that is

$$\mathbf{A}_{j\to i}(m_i, m_j) = \begin{pmatrix} \alpha_0\, (m_i/m_j)^{s_Q} \\ \delta_0\, (m_j/m_i)^{r_Q} \end{pmatrix} \quad \text{for pure mutual assessment.} \tag{3.4}$$

Importantly, any combination of these modes of assessment can be expressed by the assessment function $\mathbf{A}_{j\to i}$, and this allows the description of animal contests that do not follow a pure assessment strategy [14].

Representing the attractive and repulsive components of equation (2.1) as a two-element vector $\mathbf{V}_0$,

$$\mathbf{V}_0(x_{ij}) = \begin{pmatrix} \exp(\ \ \beta x_{ij}^2) \\ \ln(x_{ij}) \end{pmatrix}, \tag{3.5}$$

we can conveniently express $V_{j\to i}$ as the dot product of equations (3.2) and (3.5),

$$V_{j\to i}(x_{ij}) = \mathbf{A}_{j\to i}(m_i, m_j) \cdot \mathbf{V}_0(x_{ij}). \tag{3.6}$$

This separation of contest behaviour into two functional components, a system-specific component that encodes the contestant's assessment strategy ($\mathbf{A}_{j\to i}$) and a more generic component that encodes the spatial properties of the contest interaction ($\mathbf{V}_0$), is an important feature of our model.

In figure 3, equations (3.3) (3.6) are used to plot the potentials $V_{i\to j}$ and $V_{j\to i}$ under pure self-assessment (equation (3.3) with $s = 1$) and pure mutual assessment (equation (3.4) with $s_Q = 1$ and $r_Q = 2$), for the interactions of small size-matched contestants, a small contestant with a large contestant, and large size-matched contestants. The differences between these assessment strategies are immediately apparent when comparing their respective interaction potentials. Notably, the self-assessment potentials vary with the absolute values of m_i and m_j, while the mutual assessment potentials depend only on the size ratio m_i/m_j. This makes mutual assessment scale-invariant (the effective interaction potentials of size-matched contestants are independent of size, compare figure 3*a* and *c*), but very sensitive to size difference, as evident by the pronounced broken symmetry between $V_{j\to i}$ and $V_{i\to j}$ for the interaction of unmatched contestants (figure 3*b*).

3.2. Accounting for fighting costs

The RHP is in general time-dependent, as it reflects the current state of a contestant. For example, injured or energy-depleted individuals would have a decreased RHP compared with their uncompromised state. Direct costs of fighting come in two main forms: (i) self-inflicted costs (due to a contestant's own actions) and (ii) costs inflicted by the rival. The contributions of these costs to the contestants' decision-making have been previously considered as a feature of the assessment strategy [11]. In particular, pure self-assessment models assume that the rival's actions do not inflict costs, while in mutual assessment (as well as in 'cumulative assessment' [9], which we do not explore here) both self- and rival-inflicted costs are integrated [11].

Here, we extend the model to account for these two main costs, but note that the following approach can be used, in principle, to account for any cost. We set the total self-inflicted cost and the total rival-inflicted cost as increasing functions of the accumulated contest time t_σ

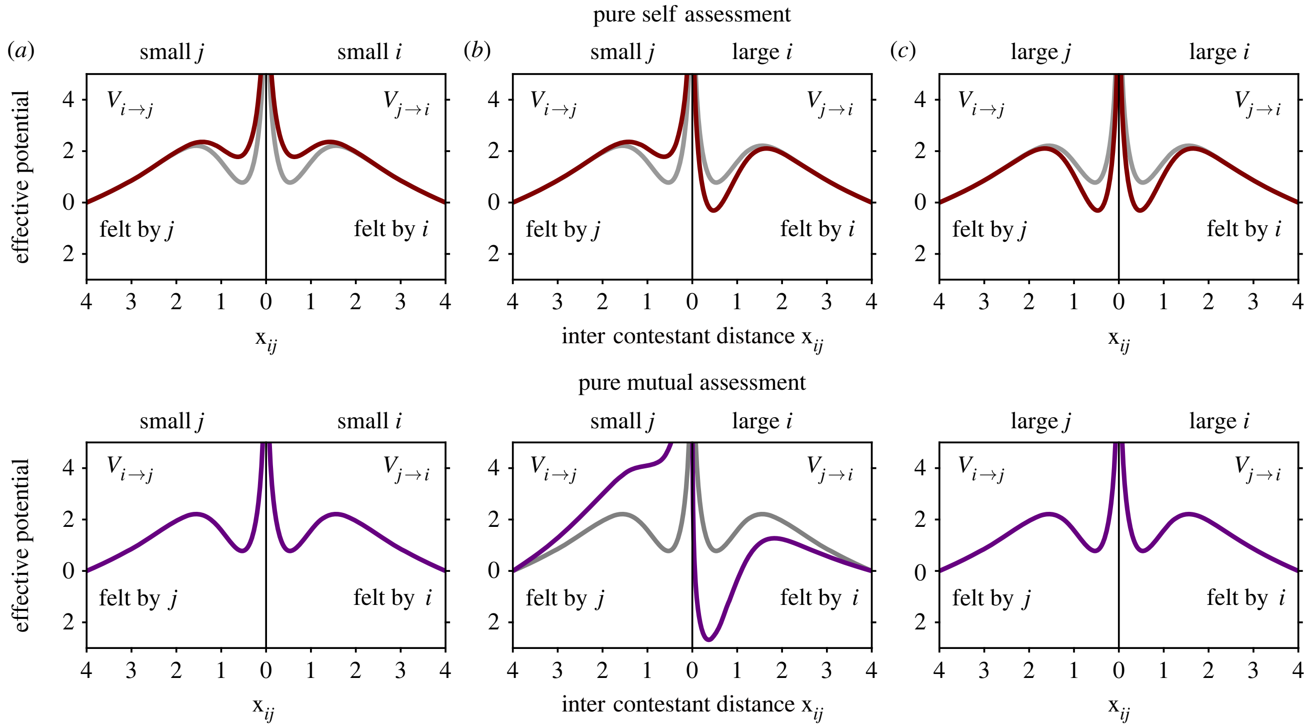

Figure 3. Assessment strategies in terms of contestant interaction potentials. By expressing an assessment strategy in terms of how the interaction parameters $\alpha_{j\to i}$ and $\delta_{j\to i}$ of equation (2.1) vary with the contestants' effective sizes, as described in equations (3.1)–(3.6), we map these behavioural categories into the interaction potentials of the contestants. Under pure self-assessment (equation (3.3) with $s = 1$) and pure mutual assessment (equation (3.4) with $s_Q = 1$ and $r_Q = 2$), the potentials $V_{i\to j}$ and $V_{j\to i}$ are shown for the interaction of small size-matched contestants ($m_j = m_i = 0.8$, (*a*)), a small contestant with a large contestant ($m_j = 0.8$, $m_i = 1.2$ for self-assessment, and $m_j = 0.9$, $m_i = 1.1$ for mutual assessment, (*b*)), and large size-matched contestants ($m_j = m_i = 1.2$, (*c*)). For reference, each graph also shows the potentials of medium size-matched contestants ($m_j = m_i = 1$) in grey. Equations (3.3) and (3.4) were used with $\alpha_0 = 7$ and $\delta_0 = 3$.

and model the dependence of the effective size on these costs as

$$m_i(t_\sigma) = \frac{\mu_i}{1 + C_i(t_\sigma) + C_{j\to i}(t_\sigma)}, \tag{3.7}$$

where μ_i is the effective size of contestant i before the contest had started, C_i is the accumulated self-inflicted cost and $C_{j\to i}$ is the accumulated cost inflicted by the rival j. As a proof of concept, we write simple but useful expressions for C_i and $C_{j\to i}$ as

$$C_i(t_\sigma) = K_{\text{self}}\, t_\sigma \quad \text{and} \quad C_{j\to i}(t_\sigma) = K_{ij}\,\frac{\mu_j}{\mu_i}\, t_\sigma, \tag{3.8}$$

where K_{self} and $K_{ij}\,\mu_j/\mu_i$ are the rates at which their respective costs are accrued. Equation (3.8) naively assumes that costs are incurred continuously and deterministically, and that the rate of incurring self-inflicted costs is independent of the contestant's own effective size. Furthermore, it assumes that the rate of incurring costs from the rival is proportional to the initial effective size ratio   such that the larger contestant inflicts costs faster but incurs them slower. Importantly, the integration of costs into the model, using equation (3.7), is not predicated on these simplifying assumptions. Combining equations (3.7) and (3.8), the resulting expressions for m_i and m_j during the contest are

$$m_i(t_\sigma) = \frac{\mu_i}{1 + \left(K_{\text{self}} + K_{ij}\,\dfrac{\mu_j}{\mu_i}\right) t_\sigma},$$

$$m_j(t_\sigma) = \frac{\mu_j}{1 + \left(K_{\text{self}} + K_{ij}\,\dfrac{\mu_i}{\mu_j}\right) t_\sigma}. \tag{3.9}$$

While both m_i and m_j decrease monotonically with t_σ, when $\mu_i > \mu_j$ and $K_{ij} \neq 0$ (e.g. in an asymmetric contest with mutual assessment), the ratio m_i/m_j increases and approaches a constant as $t_\sigma \to \infty$ (electronic supplementary material, S5). The dynamics of m_i, m_j and m_i/m_j according to equation (3.9) is shown with only self-inflicted costs ($K_{ij} = 0$) in figure 4*a*, and with both self-inflicted and rival-inflicted costs ($K_{ij} \neq 0$) in figure 4*b*.

The dependence of the effective sizes on t_σ due to costs means that the interaction potentials themselves depend on t_σ through equation (3.6), as demonstrated in figure 4*c*,*d*. This ultimate manifestation of costs in the model has a straightforward behavioural interpretation: the accumulation of costs affects the internal motivation of the contestants to fight and/or their perception of the opponent, and therefore alters the nature of their interaction. In pure self-assessment, self-inflicted costs lead to simultaneous reduction in the effective attraction of both contestants towards their rival, as evident by the diminishing potential wells of figure 4*c*. In mutual assessment, rival-inflicted costs increase the asymmetry of the interaction, as captured by the opposing trends of the potentials in figure 4*d*. The relative contest potentials vary accordingly with t_σ, as shown in figure 4*e*,*f*. For both cases studied here   pure self-assessment (equation (3.3) with $s = 1$) and pure mutual assessment (equation (3.4) with $s_Q = 1$ and $r_Q = 2$)   the bounding well of V_{contest}, which defines the contest regime, becomes less attractive (shallower) as the contest proceeds. In figure 4*e*, this trend eventually leads to contest termination, as the bounding well disappears and V_{contest} becomes strictly repulsive.

4. Trends of contest duration

The duration of contests is widely used as a readily observable and relatively unbiased measure of contest dynamics.

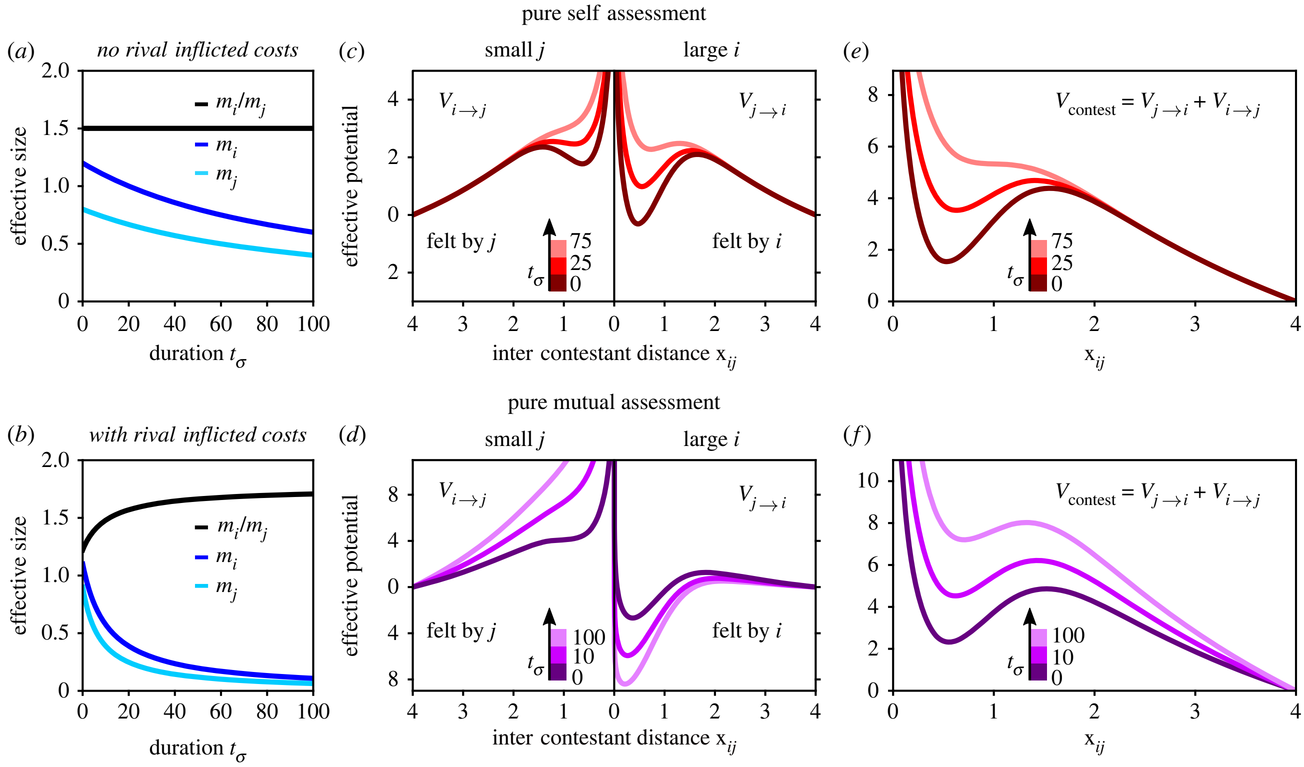

Figure 4. Effects of fighting costs. (*a*,*b*) The dynamics of the effective sizes m_i, m_j and of the ratio m_i/m_j, according to equation (3.9). (*a*) With only self-inflicted costs ($K_{ij} = 0$), where $K_{\text{self}} = 0.01$, and with initial effective sizes $\mu_i = 1.2$ and $\mu_j = 0.8$. (*b*) With both self-inflicted and rival-inflicted costs ($K_{ij} \neq 0$), where $K_{\text{self}} = 0.01$ and $K_{ij} = 0.1$, and with initial effective sizes $\mu_i = 1.1$ and $\mu_j = 0.9$. (*c*,*d*) The dependence of m_i and m_j on the accumulated contest duration t_σ due to costs means that the interaction potentials themselves depend on t_σ. Here, the potentials $V_{i\to j}$ and $V_{j\to i}$ vary according to the values of m_i and m_j in *a* (*c*) and *b* (*d*) as t_σ increases. Note that in *d*, the asymmetry between $V_{i\to j}$ and $V_{j\to i}$ increases with t_σ, in accordance with the trend of m_i/m_j in *b*. (*e*,*f*) The relative contest potential vary accordingly with t_σ, such that the bounding well that defines the contest regime becomes less attractive (shallower).

Many behavioural studies examine the relation between contest duration and the RHP of the contestants in order to determine whether a given species tends to settle contests through self- or mutual assessment [11,13,14]. Notably, pure self-assessment models predict that contest duration would generally increase with the mean RHP of the contestants [12], as the persistence of purely self-assessing contestants is determined by their absolute RHP. By contrast, mutual assessment models predict contest duration to strongly decrease with the contestants' RHP ratio, and that the duration of RHP-matched contests would not scale with RHP at all [12]. Here, we show that the same trends can be derived and understood within our model using a physics-inspired reasoning of 'contestant particles' escaping a potential well.

When deriving these trends, we consider two limiting cases in terms of fighting costs. In the 'no-cost' limit, the costs accumulated during the course of a single contest are negligible. This means that the effective sizes m_i and m_j do not change during the contest, making V_{contest} effectively independent of contest duration. Although not realistic, the no-cost limit sets a useful upper bound on contest duration. In the opposing 'cost-driven' limit, a single contest entails very significant costs, resulting in m_i and m_j decaying substantially during the contest, and in a corresponding dependence of V_{contest} on contest duration as illustrated in figure 3*e*,*f*. The termination of a no-cost contest is noise-driven entirely governed by the stochastic component of the contestants' motion and the shape of V_{contest}, while the duration of a cost-driven contest is dominated by the accrued costs, as described below.

In the context of the model, contest duration can be thought of as the time it takes for the contestants to escape the potential well of V_{contest} once they are trapped by its transient bounded state. The effective 'contest bounding energy', U, can be obtained for any mode of assessment (electronic supplementary material, S6) as a function of m_i and m_j,

$$U(m_i, m_j) = [V_{\text{contest}}(x_\cap) \quad V_{\text{contest}}(x_\cup)]_{m_i, m_j}, \tag{4.1}$$

where note that V_{contest}, as well as $x_\cap$ and $x_\cup$, depend on m_i and m_j through equation (3.2). Figure 5*a*,*b* illustrates the dependence of U on m_i and m_j in pure self- and pure mutual assessment. Notably, in pure self-assessment U increases with the sum of the effective sizes (for $s \neq 1$ in equation (3.3), U increases with the power sum $m_i^s + m_j^s$), whereas in pure mutual assessment, U depends only on the effective size ratio, and decreases as m_i/m_j increases (for proper values of s_Q and r_Q in equation (3.4), e.g. for the chosen values of $s_Q = 1$ and $r_Q = 2$; see electronic supplementary material, S7).

In the no-cost case, contest dynamics are analogous to the dynamics of Brownian particles in an energy trap of constant depth U [44]. Then the mean contest duration, t_c, should increase exponentially with U,

$$t_c = \Pi \exp\left(\frac{U(m_i, m_j)}{T_{\text{eff}}}\right), \tag{4.2}$$

where the pre-exponential factor Π is assumed to vary weakly with m_i and m_j such that the exponential dictates the qualitative trend of t_c, and T_{eff} is the 'effective temperature' of the contestant particles' interaction. Equation (4.2) relies on the assumption that, once within the contest range, the contestants reach the minimum of V_{contest}

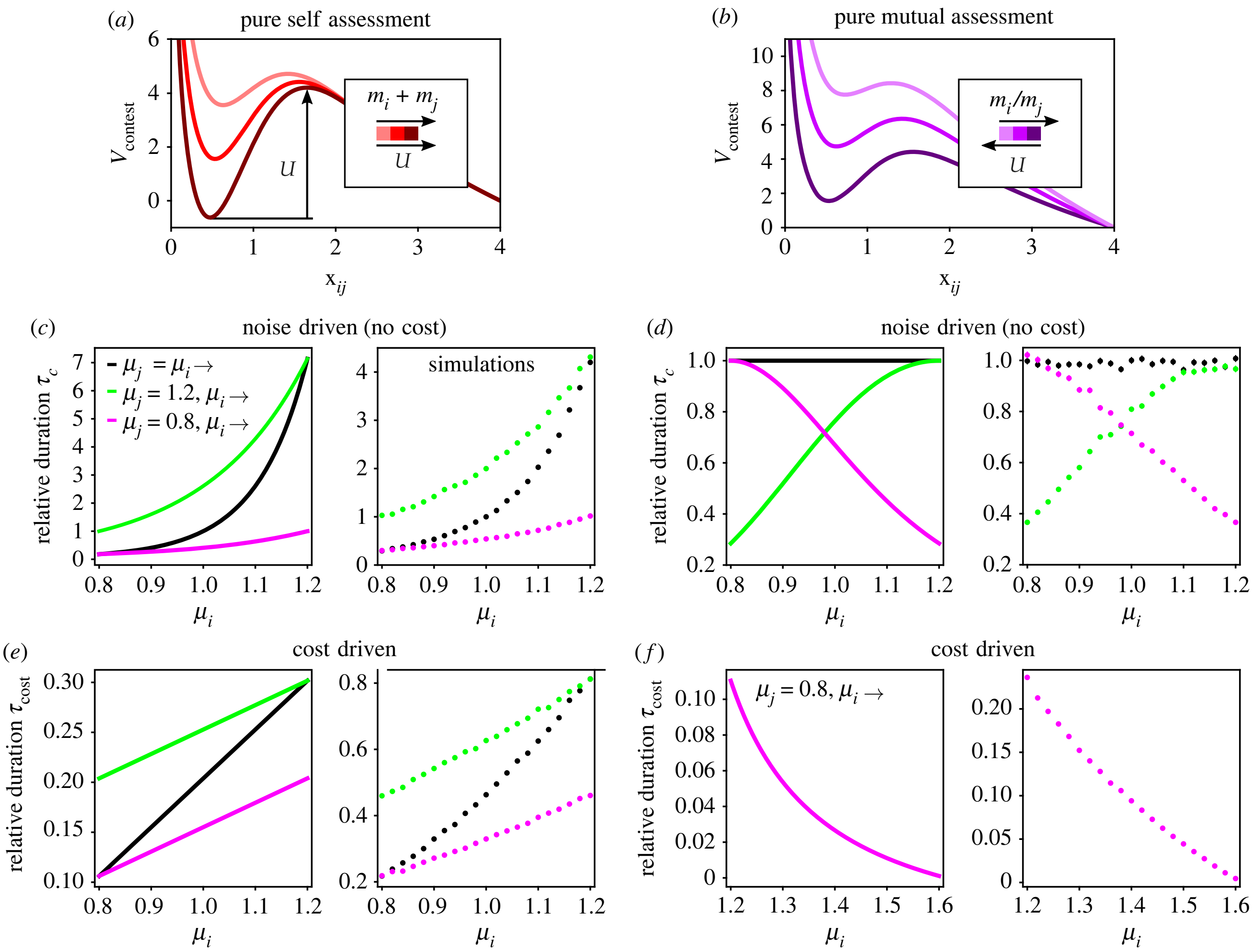

Figure 5. Trends of contest duration. (*a*,*b*) The dependence of the effective 'contest bounding energy' U on m_i and m_j in pure self- and pure mutual assessment. (*c*–*f*) Three trends of contest duration with respect to the initial effective sizes μ_i and μ_j are examined in the model for pure self- and pure mutual assessment: (i) Increasing size in size-matched contests ($\mu_j = \mu_i \rightarrow$), (ii) increasing size of smaller contestant in asymmetric contests ($\mu_j = 1.2,\ \mu_i \rightarrow$), and (iii) increasing size of larger contestant in asymmetric contests ($\mu_j = 0.8,\ \mu_i \rightarrow$). The left graph of each panel shows the qualitative theoretical trends calculated according to equations (4.1)–(4.3) with $\Pi = \Pi^\star = 1$ and $T_{eff} = 2D = 1$ (see also electronic supplementary material, S6 and S8), and the right graph shows the mean trends in simulations ($n = 5000$, error bars show SEM). (*c*,*d*) Noise-driven contest termination, where m_i and m_j remain the same during the contest, and therefore $V_{contest}$ is independent of contest duration. (*e*,*f*) Cost-driven contest termination, where the decay of m_i and m_j during the contest is governed by equation (3.9). The cost rates are $K_{self} = 0.2$, $K_{ij} = 0$ in (*e*) and $K_{self} = 0.01$, $K_{ij} = 0.3$ in (*f*). In (*f*), μ_i is varied in the range where the analytic expression for the cost-driven duration is valid (electronic supplementary material, S8), given that $\mu_j = 0.8$.

quickly within an average time that is significantly shorter than t_c and spend the rest of the contest near the minimum until they escape, as in figure 2*b*.

In the cost-driven case, the cost-dominated contest duration, denoted t_{cost} henceforth, can be obtained by considering the decay of the effective sizes due to costs up to the point where $V_{contest}$ is no longer attractive, as illustrated in figure 4*e*. This happens when the two extrema of $V_{contest}$ merge into a single inflection point, which for our particular choice of interaction potentials satisfies the condition (electronic supplementary material, S1)

$$\frac{\alpha_{j\rightarrow i} + \alpha_{i\rightarrow j}}{\delta_{j\rightarrow i} + \delta_{i\rightarrow j}} = \frac{e}{2}, \tag{4.3}$$

where e is Euler's number. Together with equations (3.2) and (3.9), the condition of equation (4.3) can be invoked to evaluate t_{cost} for any mode of assessment. In electronic supplementary material, S8, we derive analytic expressions for t_{cost} under pure self-assessment and pure mutual assessment, which are valid estimates when the costs are large enough to make t_{cost} much smaller than the noise-driven duration t_c.

Since we are interested in the trends of contest duration with respect to m_i and m_j under a particular assessment strategy, and since absolute durations vary between species, it is useful to define relative durations as $\tau_c = t_c/t_c^\star$ and $\tau_{cost} = t_{cost}/t_c^\star$, with $t_c^\star = \Pi^\star \exp(U^\star/T_{eff})$, where $\Pi^\star$ and $U^\star$ correspond to a no-cost contest between two size-matched contestants of the reference effective size ($m_i = m_j = 1$, recall equation (3.1)), for which all modes of assessment described by equation (3.2) yield identical interaction potentials, and therefore the same mean contest duration $t_c^\star$.

We examine three trends of contest duration with respect to the initial effective sizes, μ_i and μ_j, for pure self- and pure mutual assessment: (i) increasing size in size-matched contests, (ii) increasing size of the smaller contestant in asymmetric contests, and (iii) increasing size of the larger contestant in asymmetric contests, as described in figure 5*c* *f*. The theoretical trends predicted by equations (4.1) (4.3) are in agreement with the mean trends obtained from simulations, and are aligned with previously reported experimental trends and predictions of game-theoretic models [11,14]. This demonstrates that contest duration can be derived directly from the underlying physical properties of the interaction, as an emergent feature of contest dynamics. Comparison between the no-cost trends (figure 5*c*,*d*) and the cost-driven trends (figure 5*e*,*f*) shows that both cases give rise to the same qualitative trends suggesting that explicit integration of fighting costs (which relies on a cost function that typically cannot be measured) is not necessary to explain these previously observed trends.

5. Properties of asymmetric contests

5.1. Dynamics of asymmetric contests

Interactions between unmatched contestants are characterized by broken symmetry. Here, we explore in the model the effects of this asymmetry on the spatio-temporal dynamics of the contest and the emergence of chase dynamics a ubiquitous feature of animal contests. As illustrated in figure 6*a* for strongly asymmetric interaction potentials, within the 'chase' range the larger contestant is attracted by a deep minimum leading it to move towards its smaller rival, while the smaller contestant is repelled in the same direction moving away from its larger rival. Together, these effects gives rise to directed chase behaviour during the contest, where the larger contestant tends to chase its smaller rival away. The extent to which a contest is dominated by chase dynamics is determined by the magnitude of asymmetry between the inter-contestant effective forces, measured by

$$\Delta F_{ij}(x_{ij}) = F_{i\to j}(x_{ij}) \quad F_{j\to i}(x_{ij}). \tag{5.1}$$

In particular, since contests are governed by the forces near the minimum of V_{contest}, the extent of chase dynamics during a contest is determined by $\Delta F_{ij}(x_{\cup})$. Figure 6*b* shows ΔF_{ij} as a function of x_{ij} for strongly unmatched contestants (left) and $\Delta F_{ij}(x_{\cup})$ as a function of the larger contestant's effective size m_i (right) under pure self-assessment (equation (3.3) with $s = 1$) and pure mutual assessment (equation (3.4) with $s_Q = 1$ and $r_Q = 2$). This comparison further illustrates that in mutual assessment, a relatively small effective size difference is translated into strong interaction asymmetry.

To quantify chase dynamics in the contestants' trajectories, we consider the direction correlation between the velocity of the contestants' midpoint measured by $\hat{\mathbf{v}}_{\text{m}}$, and the inter-contestant direction $\hat{\mathbf{x}}_{ij}$, as defined in figure 6*c* (inset). The temporal mean of this 'chase correlator', denoted by $\langle\hat{\mathbf{v}}_{\text{m}}\cdot\hat{\mathbf{x}}_{ij}\rangle$, is theoretically zero for symmetric interactions, but positive for asymmetric interactions because of the directional bias imposed by the asymmetry, and approaches 1 if the interaction is dominated by the chase phase.

Figure 6*c*,*d* compare typical trajectories of strongly asymmetric and symmetric contests (under pure mutual assessment) in simulations. While the trajectories of symmetric contests are scrambled and relatively localized, the trajectories of strongly asymmetric contests feature substantial directional alignment and persistence, and consequently much greater displacement, due to chase dynamics. Figure 6*e* shows the chase correlator $\langle\hat{\mathbf{v}}_{\text{m}}\cdot\hat{\mathbf{x}}_{ij}\rangle$ as calculated from simulations, where x_{ij} and m_i are varied as in figure 6*b*. Evidently, the trends of $\langle\hat{\mathbf{v}}_{\text{m}}\cdot\hat{\mathbf{x}}_{ij}\rangle$ mirror the trends of ΔF_{ij}, suggesting that the relation between $\langle\hat{\mathbf{v}}_{\text{m}}\cdot\hat{\mathbf{r}}_{ij}\rangle$ and ΔF_{ij} follows simple (linear) scaling within almost the entire contest range and for a wide range of asymmetries.

5.2. Contest outcome and size-related advantage

The ultimate expression of the RHPs is the outcome of the contest, wherein the winner obtains the resource. In the model, the resource is well-defined as the global minimum of the effective resource potential, and the outcome of the contest is determined when one of the contestants reaches the resource after the contest has ended. The advantage of larger effective size can be, therefore, examined directly in the model. In figure 7, we demonstrate for pure mutual assessment (equation (3.4) with $s_Q = 1$ and $r_Q = 2$) how interaction asymmetry increases the winning probability of the larger contestant further showcasing the scope of the model in the describing observable contest dynamics.

We consider 'fair start' contests (figure 7*a*), which start when the contestants reach the contest range at equivalent vantage points with respect to the resource such that neither of them has an initial positional advantage. Any advantage at winning such contests would, therefore, emerge from the dynamics of the contest itself. In figure 7*b*, we examine how the distribution of the contestants' positions at the end of the contest is affected by the size asymmetry. As the size asymmetry increases, contests increasingly end with the larger contestant at positional advantage with respect to the resource ($|\theta| < 90°$, see upper panel in figure 7*b*). This effect is due to increasing chase dynamics, in which the larger contestant tends to chase its rival away from the resource leaving the larger contestant closer to the resource when the contest terminates. Figure 7*c* compares the probability that the larger contestant is closer to the resource at the end of the contest with the probability that it is the winner, as a function of the size ratio. The match between these probabilities means that in the model's simulations, the positional configuration at the end of the contest determines its outcome, where the contestant closer to the resource becomes the winner.

6. Discussion

The study of animal contests has a rich history, extending back to the first formal application of evolutionary stable strategies to explain the evolutionary logic of these agonistic interactions [2,45]. In the following decades, game-theoretic models have yielded great insights into animal contests across taxonomic boundaries and contexts [1,46]. Nevertheless, the scarcity of direct empirical evidence in support of these models highlights the limitations of game-theoretic approaches in the study of animal contests [12 14]. In particular, the difficulty of measuring contest dynamics as modelled within game theory has been a topic of recent discussion and debate [12,14,20 22]. One inherent barrier in the correspondence between theory and experiment has been the omission of within-contest dynamics by game-theoretic models, which typically verify their underlying decision rules based on contest endpoints.

In this work, we developed a new theoretical framework for animal contest dynamics based on measurable spatio-temporal characteristics of contest behaviour. The basic building blocks of our model are effective interaction potentials,

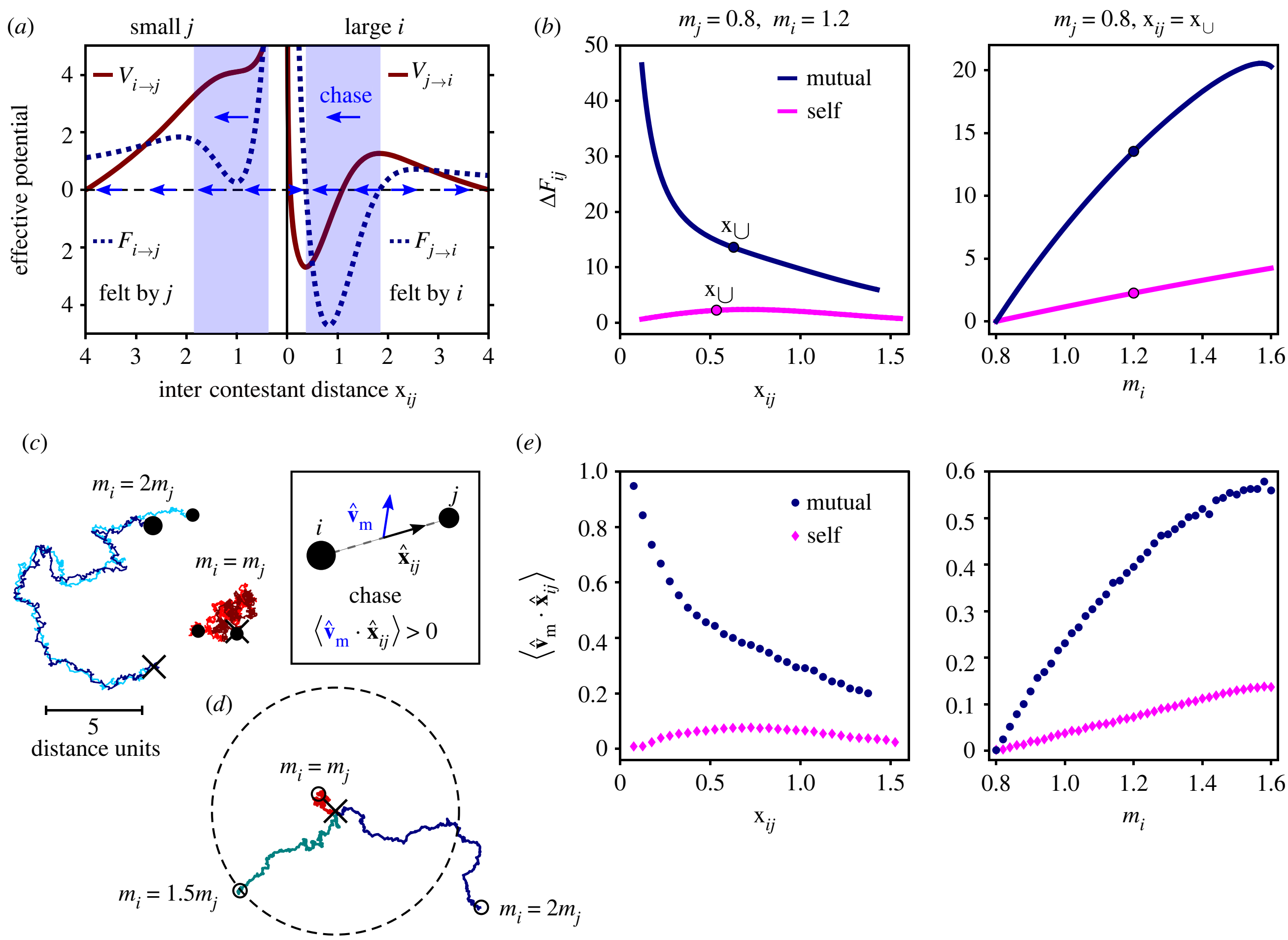

Figure 6. Interaction asymmetry and chase dynamics. (*a*) Strongly asymmetric interaction potentials illustrate how interaction asymmetry leads to chase dynamics. Shaded rectangles mark the chase range, within which the larger contestant is attracted by a deep minimum, while the smaller contestant is repelled in the same direction. Arrows indicate the direction of motion for each contestant, as dictated by the signs of the forces $F_{j\to i}$ and $F_{i\to j}$. (*b*) Force asymmetry $\Delta F_{ij} = F_{i\to j} - F_{j\to i}$ as a function of x_{ij} for strongly unmatched contestants (left) and $\Delta F_{ij}(x_\cup)$ (at the minimum of $V_{contest}$) as a function of the larger contestant's effective size m_i (right) under pure self-assessment (equation (3.3) with $s = 1$) and pure mutual assessment (equation (3.4) with $s_Q = 1$ and $r_Q = 2$). Circles mark equivalent points in both graphs. (*c*) Typical trajectories of strongly asymmetric and symmetric contests in simulations. Chase dynamics is quantified by the temporal mean of the direction correlation between $\hat{\mathbf{v}}_m$ and $\hat{\mathbf{x}}_{ij}$, as defined in the inset. (*d*) Trajectories of the contestants' midpoint during contests under pure mutual assessment for different effective size ratios. These trajectories, of equal durations, demonstrate the effect of chase dynamics on the contestants' displacement during the contest. In (*c*,*d*), the 'X' marks the contestants' midpoint at the contest onset and the circles mark final positions. (*e*) The 'chase correlator' $\langle \hat{\mathbf{v}}_m \cdot \hat{\mathbf{x}}_{ij} \rangle$ as calculated from simulations ($n = 5000$) under pure self-assessment and pure mutual assessment, where x_{ij} and m_i are varied as in (*b*).

which encode generic rules of inter-contestant motion through the effective interaction forces that they generate. Importantly, these rules of motion can be directly extracted from empirical measurements of contest trajectories, and the simulated contest dynamics that our model gives rise to can be directly compared with the observable dynamics of real contests. Our approach requires few *a priori* assumptions about the observed interactions and is not predicated on decision rules imposed by a specific assessment strategy. Moreover, it has greater applicability to the study of contests in natural conditions, because it can use the entire information provided by the contestants' trajectories and does not critically rely on the ability to measure contest duration. Our approach is, therefore, robust to partially sampled contests, in which the observer may be unsure of the onset of the contest, where the contestants may move out of sight, or when contests are prematurely ended by an external stimulus.

Once the basic form of the effective interaction potentials has been established, our framing of assessment strategies as variations of the interaction parameters depending on the contestants' RHPs, as represented by the assessment function, allows the exploration of various strategies along the assessment continuum. This includes strategies that do not fall into the self- or mutual assessment categories, such as mixed assessment strategies [14]. Our model's representation of assessment strategies also brings them into the measurable domain where, rather than being retrospectively assigned based on the eventual contest outcome, the assessment strategy can in principle be inferred from the way the interaction varies with the contestants' RHPs. More broadly, modelling approaches that relate the measurable nature of the interaction to the current state of the contestants can be extended to encompass other determinants of behaviour, such as prior fighting experience (winner and loser effects, [47]), as we have demonstrated in our implementation of fighting costs.

While our model offers a new way of deriving and understanding previously described strategy-dependent trends of contest duration as a function of the contestants' RHPs, the detailed description of the contestants' spatial dynamics allows us to go far beyond paraphrasing the predictions of

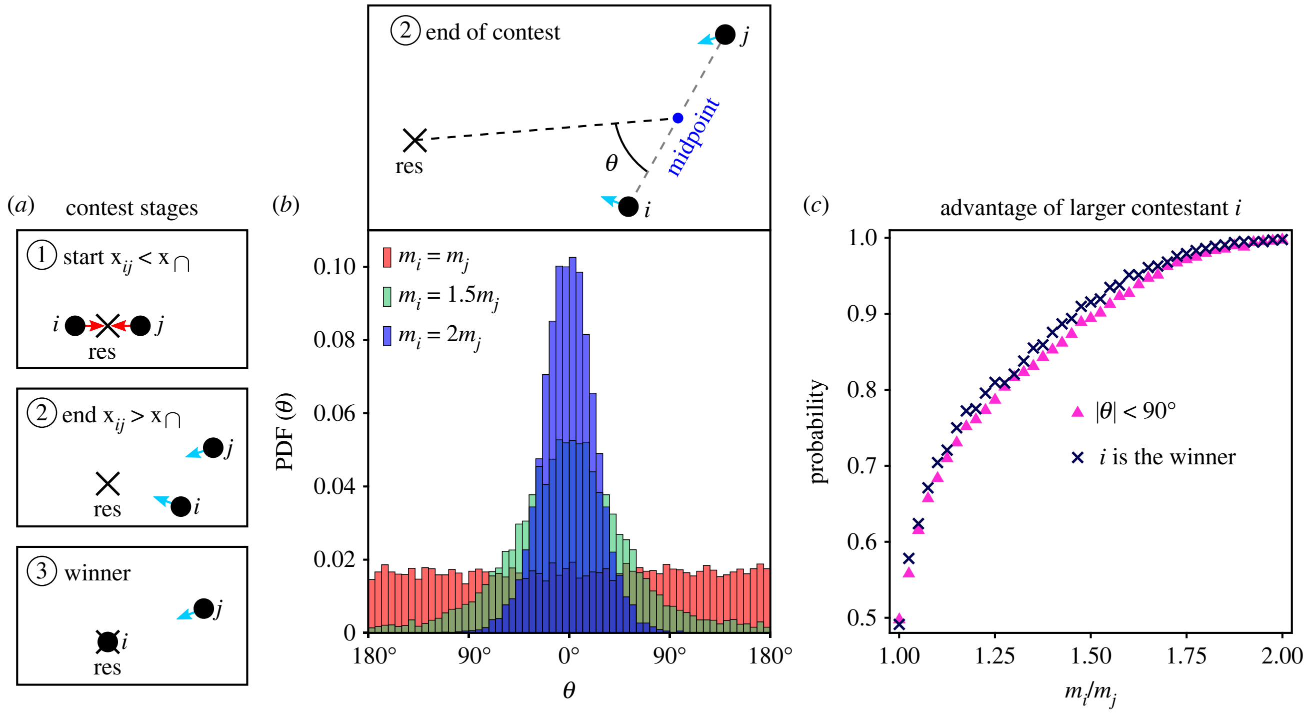

Figure 7. Winning the contest. (*a*) The stages of a 'fair start' contest, which starts with the contestants at equivalent vantage points with respect to the resource—as in ①, ends at some configuration—as in ②, and subsequently its outcome (winner) is determined when one of the contestants reaches the resource—as in ③. (*b*) The positional advantage of contestant *i* with respect to the resource at the end of the contest can be quantified by the angle θ, as defined in the upper panel. When $|\theta| > 90°$, *i* is closer to the resource than *j*. The lower panel shows the distribution of θ under pure mutual assessment (equation (3.4) with $s_Q = 1$ and $r_Q = 2$) for different effective size ratios. The bias towards $\theta = 0°$ increases with effective size asymmetry due to increasing chase dynamics, where *i* chases *j* away from the resource. (*c*) Comparison between the probability that the larger contestant *i* is closer to the resource at the end of the contest ($|\theta| < 90°$) and the probability that *i* is the winner, as a function of the size ratio. In (*b*,*c*), $n = 10\,000$ simulations for each effective size ratio.

other models. We showcased some of these applications by exploring spatio-temporal properties of asymmetric contests, notably the emergence of chase dynamics and their contribution to size-related advantage. Although we considered here only the archetypal contest scenario of two contestants that compete over a single resource, our framework can be used to describe the interactions between many contestants, various distributions of multiple resources, and even consumable resources (through a time dependence of the resource potentials). These applications are especially useful to the study of complex competitive scenarios, for example systems in which the density of contestants is variable and affects the degree to which size (or any other proxy for RHP) provides a competitive advantage [30], or systems in which many contestants move in a field of consumable resources where population-level measures could be used to explore the system's dynamics.

Furthermore, the ability to extract effective interaction potentials directly from contest trajectories offers a robust method for detecting changes within an interaction over time. This can be done by sampling the trajectories of the same contestants at different times for example by dissecting the contests into their initial and terminal stages, or by separately analysing consecutive contests among the same rivals in the same or in different conditions. Such data can be used to determine how strategies update over time or context, which has been previously discussed as a useful contribution to the understanding of assessment strategies [14]. More generally, by monitoring the detailed dynamics of contests, we can study the role that injuries, energetic expenditure, learning from prior experience or an intrinsic change in motivation play in the behavioural outputs of contestants, and thereby gain insights into the mechanisms that underlie these outputs [48]. The above suggests many further applications of our modelling approach, which we leave for future work.

With the rapid development of tools to gather extremely high-resolution data on behavioural interactions in both laboratory [49,50] and field settings [24,51], our model aims to bridge the growing gap between empirical capabilities and theory. Not only can the model recapitulate many predictions of previous models, but, importantly, it enables the description of realistic and detailed contest dynamics within observable time scales. Our theoretical framework should, therefore, facilitate new approaches and insights in the study of this widespread aspect of animal behaviour.

Data accessibility. All data and modelling information essential to this theoretical study are included in the article and/or electronic supplementary material. Code and simulated trajectories are also provided in the following Zenodo: https://doi.org/10.5281/zenodo.7377238 [52] (see electronic supplementary material, S4). Further data or code requests will be happily fulfilled by the authors.

The data are provided in electronic supplementary material [53].

Authors' contributions. A.H.: conceptualization, formal analysis, investigation, methodology, software, validation, visualization, writing original draft, writing review and editing; A.J.: conceptualization, funding acquisition, supervision, writing original draft, writing review and editing; N.S.G.: conceptualization, funding acquisition, investigation, methodology, supervision, writing original draft, writing review and editing.

All authors gave final approval for publication and agreed to be held accountable for the work performed therein.

Conflict of interest declaration. We declare we have no competing interests.

Funding. This work was supported by a Minna James Heineman Stiftung research grant (to A.J.).

References

1. Briffa M, Hardy IC. 2013 Introduction to animal contests. In *Animal contests*, pp. 1–4. Cambridge, UK: Cambridge University Press.
2. Smith J, Price GR. 1973 The logic of animal conflict. *Nature* **246**, 15–18. (doi:10.1038/246015a0)
3. Smith JM. 1974 The theory of games and the evolution of animal conflicts. *J. Theor. Biol.* **47**, 209–221. (doi:10.1016/0022-5193(74)90110-6)
4. Parker GA. 1974 Assessment strategy and the evolution of fighting behaviour. *J. Theor. Biol.* **47**, 223–243. (doi:10.1016/0022-5193(74)90111-8)
5. Smith JM, Parker GA. 1976 The logic of asymmetric contests. *Anim. Behav.* **24**, 159–175. (doi:10.1016/S0003-3472(76)80110-8)
6. Parker GA. 1979 Sexual selection and sexual conflict. In *Sexual selection and reproductive competition in insects* (eds MS Blum, NA Blum), pp. 123–166. New York, NY: Academic Press.
7. Enquist M, Leimar O. 1983 Evolution of fighting behaviour: decision rules and assessment of relative strength. *J. Theor. Biol.* **102**, 387–410. (doi:10.1016/0022-5193(83)90376-4)
8. Payne RJ, Pagel M. 1997 Why do animals repeat displays? *Anim. Behav.* **54**, 109–119. (doi:10.1006/anbe.1996.0391)
9. Payne RJ. 1998 Gradually escalating fights and displays: the cumulative assessment model. *Anim. Behav.* **56**, 651–662. (doi:10.1006/anbe.1998.0835)
10. Kokko H. 2013 Dyadic contests: modelling flights between two individuals. In *Animal contests* (eds IC Hardy, M Biffa), pp. 5–32. Cambridge, UK: Cambridge University Press.
11. Arnott G, Elwood RW. 2009 Assessment of fighting ability in animal contests. *Anim. Behav.* **77**, 991–1004. (doi:10.1016/j.anbehav.2009.02.010)
12. Taylor P, Elwood RW. 2003 The mismeasure of animal contests. *Anim. Behav.* **65**, 1195–1202. (doi:10.1006/anbe.2003.2169)
13. Pinto NS, Palaoro AV, Peixoto PE. 2019 All by myself? Meta-analysis of animal contests shows stronger support for self than for mutual assessment models. *Biol. Rev.* **94**, 1430–1442. (doi:10.1111/brv.12509)
14. Chapin KJ, Peixoto PEC, Briffa M. 2019 Further mismeasures of animal contests: a new framework for assessment strategies. *Behav. Ecol.* **30**, 1177–1185. (doi:10.1093/beheco/arz081)
15. Payne RJ, Pagel M. 1996 Escalation and time costs in displays of endurance. *J. Theor. Biol.* **183**, 185–193. (doi:10.1006/jtbi.1996.0212)
16. Mesterton-Gibbons M, Marden JH, Dugatkin LA. 1996 On wars of attrition without assessment. *J. Theor. Biol.* **181**, 65–83. (doi:10.1006/jtbi.1996.0115)
17. Enquist M, Leimar O, Ljungberg T, Mallner Y, Segerdahl N. 1990 A test of the sequential assessment game: fighting in the cichlid fish *Nannacara anomala*. *Anim. Behav.* **40**, 1–14. (doi:10.1016/S0003-3472(05)80660-8)
18. Parker GA, Rubenstein DI. 1981 Role assessment, reserve strategy, and acquisition of information in asymmetric animal conflicts. *Anim. Behav.* **29**, 221–240. (doi:10.1016/S0003-3472(81)80170-4)
19. Hammerstein P, Parker GA. 1982 The asymmetric war of attrition. *J. Theor. Biol.* **96**, 647–682. (doi:10.1016/0022-5193(82)90235-1)
20. Parker GA. 2019 So we all choose our own assessment rules?: a comment on Chapin *et al*. *Behav. Ecol.* **30**, 1188–1188. (doi:10.1093/beheco/arz120)
21. Elwood RW. 2019 Problems with repeated contests: a comment on Chapin *et al*. *Behav. Ecol.* **30**, 1189. (doi:10.1093/beheco/arz121)
22. Leimar O. 2019 Game theory models of animal contests: are we at a standstill?: a comment on Chapin *et al*. *Behav. Ecol.* **30**, 1190–1191. (doi:10.1093/beheco/arz144)
23. Dell AI *et al.* 2014 Automated image-based tracking and its application in ecology. *Trends Ecol. Evol.* **29**, 417–428. (doi:10.1016/j.tree.2014.05.004)
24. Nathan R *et al.* 2022 Big-data approaches lead to an increased understanding of the ecology of animal movement. *Science* **375**, eabg1780. (doi:10.1126/science.abg1780)
25. Huntingford FA, Turner AK. 1987 Conflict in the animal world. In *Animal conflict* (eds FA Huntingford, AK Turner), pp. 3–12. Dordrecht, The Netherlands: Springer Netherlands.
26. Ekman P. 2009 Darwin's contributions to our understanding of emotional expressions. *Phil. Trans. R. Soc. B* **364**, 3449–3451. (doi:10.1098/rstb.2009.0189)
27. Jordan LA, Kokko H, Kasumovic M. 2014 Reproductive foragers: male spiders choose mates by selecting among competitive environments. *Am. Nat.* **183**, 638–649. (doi:10.1086/675755)
28. Emlen ST, Oring LW. 1977 Ecology, sexual selection, and the evolution of mating systems. *Science* **197**, 215–223. (doi:10.1126/science.327542)
29. Fuxjager MJ, Zhao X, Rieger NS, Marler CA. 2017 Why animals fight: uncovering the function and mechanisms of territorial aggression. In *APA handbook of comparative psychology: basic concepts, methods, neural substrate, and behavior*, vol. 1, pp. 853–875. Washington, DC: American Psychological Association.
30. Haluts A, Reyes SFG, Gorbonos D, Etheredge RI, Jordan A, Gov NS. 2021 Spatiotemporal dynamics of animal contests arise from effective forces between contestants. *Proc. Natl Acad. Sci. USA* **118**, e2106269118. (doi:10.1073/pnas.2106269118)
31. Kovalev A, Filippov AE, Gorb SN. 2021 Numerical model of the spatio-temporal dynamics in a water strider group. *Sci. Rep.* **11**, 1–12. (doi:10.1038/s41598-021-96686-w)
32. Gorbonos D, Ianconescu R, Puckett JG, Ni R, Ouellette NT, Gov NS. 2016 Long-range acoustic interactions in insect swarms: an adaptive gravity model. *New J. Phys.* **18**, 073042. (doi:10.1088/1367-2630/18/7/073042)
33. Hemelrijk CK, Hildenbrandt H. 2011 Some causes of the variable shape of flocks of birds. *PLoS ONE* **6**, e22479. (doi:10.1371/journal.pone.0022479)
34. Hemelrijk CK, Kunz H. 2004 Density distribution and size sorting in fish schools: an individual-based model. *Behav. Ecol.* **16**, 178–187. (doi:10.1093/beheco/arh149)
35. Huth A, Wissel C. 1992 The simulation of the movement of fish schools. *J. Theor. Biol.* **156**, 365–385. (doi:10.1016/S0022-5193(05)80681-2)
36. Bastien R, Romanczuk P. 2020 A model of collective behavior based purely on vision. *Sci. Adv.* **6**, eaay0792. (doi:10.1126/sciadv.aay0792)
37. Jensen P, Yngvesson J. 1998 Aggression between unacquainted pigs—sequential assessment and effects of familiarity and weight. *Appl. Anim. Behav. Sci.* **58**, 49–61. (doi:10.1016/S0168-1591(97)00097-X)
38. Tachon G, Murray AM, Gray DA, Cade WH. 1999 Agonistic displays and the benefits of fighting in the field cricket, *Gryllus bimaculatus*. *J. Insect Behav.* **12**, 533–543. (doi:10.1023/A:1020970908541)
39. Popp JW. 1987 Risk and effectiveness in the use of agonistic displays by American goldfinches. *Behaviour* **103**, 141–156. (doi:10.1163/156853987X00314)
40. Martin RA. 2007 A review of shark agonistic displays: comparison of display features and implications for shark–human interactions. *Mar. Freshw. Behav. Physiol.* **40**, 3–34. (doi:10.1080/10236240601154872)
41. Paton D, Caryl P. 1986 Communication by agonistic displays. *Behaviour* **98**, 213–239. (doi:10.1163/156853986X00973)
42. Romanczuk P, Bär M, Ebeling W, Lindner B, Schimansky-Geier L. 2012 Active Brownian particles. *Eur. Phys. J. Spec. Top.* **202**, 1–162. (doi:10.1140/epjst/e2012-01529-y)
43. Arnott G, Elwood RW. 2008 Information gathering and decision making about resource value in animal contests. *Anim. Behav.* **76**, 529–542. (doi:10.1016/j.anbehav.2008.04.019)
44. Hänggi P, Talkner P, Borkovec M. 1990 Reaction-rate theory: fifty years after Kramers. *Rev. Mod. Phys.* **62**, 251. (doi:10.1103/RevModPhys.62.251)
45. Harman O. 2011 Birth of the first ESS: George Price, John Maynard Smith, and the discovery of the lost 'Antlers' paper. *J. Exp. Zool. Part B: Mol. Dev. Evol.* **316**, 1–9. (doi:10.1002/jez.b.21377)
46. Milinski M. 1991 Competition for resources. In *Behavioural ecology*, 3rd edn. (eds JR Krebs, NB Davies), pp. 137–168. Oxford, UK: Blackwell.

47. Hsu Y, Earley RL, Wolf LL. 2006 Modulation of aggressive behaviour by fighting experience: mechanisms and contest outcomes. *Biol. Rev.* **81**, 33–74. (doi:10.1017/S146479310500686X)
48. Reichert MS, Quinn JL. 2017 Cognition in contests: mechanisms, ecology, and evolution. *Trends Ecol. Evol.* **32**, 773–785. (doi:10.1016/j.tree.2017.07.003)
49. Pereira TD *et al.* 2022 SLEAP: a deep learning system for multi-animal pose tracking. *Nat. Methods* **19**, 486–495. (doi:10.1038/s41592-022-01426-1)
50. Mathis A, Mamidanna P, Cury KM, Abe T, Murthy VN, Mathis MW, Bethge M. 2018 DeepLabCut: markerless pose estimation of user-defined body parts with deep learning. *Nat. Neurosci.* **21**, 1281–1289. (doi:10.1038/s41593-018-0209-y)
51. Francisco F, Nuehrenberg P, Jordan AL. 2020 High-resolution, non-invasive animal tracking and reconstruction of local environment in aquatic ecosystems. *Mov. Ecol.* **8**, 1–12.
52. Haluts A, Jordan A, Gov NS. 2023 Code for: extracting interaction potentials from trajectories: code and a set of 30 simulated contest trajectories. *Zenodo*. (doi:10.5281/zenodo.7377238)
53. Haluts A, Jordan A, Gov NS. 2023 Modelling animal contests based on spatio-temporal dynamics. Figshare. (doi:10.6084/m9.figshare.c.6659079)